Multi-perspective Multi-modal PoL Characterization of LEO Objects

Rithwik Neelakantan
Digantara Research and Technologies Pvt Ltd, Bengaluru, India
Sivalinga Raja Shanmugam
Digantara Research and Technologies Pvt Ltd, Bengaluru, India
Ankit Agrawal
Digantara Research and Technologies Pvt Ltd, Bengaluru, India
Latha S
Digantara Research and Technologies Pvt Ltd, Bengaluru, India
Nistala Venkat Vaishnavi Lakshmi
Digantara Research and Technologies Pvt Ltd, Bengaluru, India
Tanveer Ahmed
Digantara Research and Technologies Pvt Ltd, Bengaluru, India

ABSTRACT

The Pattern of Life (PoL) characterization of a satellite in Low Earth Orbit (LEO) is an intricate process demanding high fidelity data and robust data processing techniques. The solution to this complicated problem demands a methodology based on multiple perspectives and the ability to process, synthesize and correlate data from multiple sources of varying fidelity. Towards this objective, the current research proposes a dynamic and robust methodology to precisely characterize and synthesize PoL of satellites based on a multi-perspective multi-modal analysis, involving many aspects of a Space Domain Awareness (SDA) technological chain. First, maneuver detection from different data types such as optical observations, Two Line Elements (TLE) and state vectors is described. For the maneuver detection from optical observations, the proposed technique is built upon a hypothesis-based tracking algorithm where each hypothesis makes a claim about the source of measurement, based on its statistical distance with respect to the predicted measurement. This technique is found to be suitable for processing maneuvers near-real time as well. For the maneuver detection from TLEs, a new technique called iterative sequential moving window method is proposed. The proposed technique involves a layered analysis inside the conventional moving window method for maneuver detection and does not require a user-defined threshold to be specified for maneuver detection. The iterative sequential moving window method is extended to the analysis of state vectors as well and it is found that maneuver detection using state vectors derives more accurate information about the maneuvers compared to TLEs. Next, a post-processing of the inferences derived from maneuver detection is conducted, leading to the purpose of the maneuver and correlation with the historical trend and PoL characterization of the satellite. The applications of the proposed methodology and the techniques developed for the characterization of space objects involve efficient and unambiguous cataloging of space objects, precise maneuver characterization and the generation of predictive analytics enabling reliable, action-oriented space domain awareness.

1. INTRODUCTION AND BACKGROUND

Humanity's utilization of space in the last century has been marked by significant advancements, from satellite launches to crewed missions to the Moon. The proliferation of satellites for communication, navigation, and scientific research has resulted in exponential increase in global accessibility, technological advancement and convenience. However, the increase in satellite deployment in recent times has highlighted the urgent need for a robust space operations infrastructure. Developing a comprehensive space infrastructure is essential to ensure the safety and sustainability of future space operations. A critical requirement for this development is the ability to characterize, synthesize and evaluate the Pattern of Life (PoL) of all Resident Space Objects (RSO). A good starting point for this meticulous task would be the characterization of all active assets in the Low Earth Orbit (LEO).

Copyright © 2024 Advanced Maui Optical and Space Surveillance Technologies Conference (AMOS) – www.amostech.com

The PoL characterization of a satellite in LEO is an intricate process demanding high fidelity data and robust data processing techniques. The inferences drawn from such an analysis can be subjective, depending on the requirements of the end user. The lack of ground truth data to test the reliability of the algorithms and the lack of commonality among different perspectives, requirements and definitions of PoL characterization demand a solution based on multiple perspectives and the capability to ingest and fuse data from multiple sources of varying fidelity. In this context, the current research proposes a robust methodology to precisely characterize and synthesize PoL of satellites based on a multi-perspective multi-modal analysis. The contributions of the work are twofold: 1) the development of maneuver detection techniques ingesting multiple data types such as raw optical sensor observations, Two Line Elements (TLE) and state vectors and 2) a multi-perspective correlation and inference generation for maneuver detection, anomaly detection & threat analysis, identifying the purpose of the maneuver etc.

2. LITERATURE REVIEW

There is immense wealth of literature for detecting the maneuvers of space objects from multiple data types and using multiple techniques. A popular methodology in the literature to analyze the maneuvers from TLE data is to employ a sliding window method to evaluate the standard deviation of the time averaged motion and identify the maneuvers by determining the deviations which exceed user defined thresholds. Ref. [1] developed such a technique wherein the dispersion of a pre-defined parameter is calculated by finding the difference between its expected and actual values. The statistical distribution of this dispersion is then utilized to determine a maneuver threshold. Maneuvers are identified when the dispersions surpass this threshold. This methodology was shown to be applicable to the detection of other ‘space events’ also such as a collision event and solar activity changes. Another notable feature of the moving window technique is the computational efficiency of the numerical implementation and can be attributed to the simple cubic polynomial fitting of the sequential time series data. The sharp increase of the derivative of the time series data at the time of maneuver is also used to detect the event.

Ref. [2] employed a preprocessing algorithm to smoothen the TLE data and correlated the difference between the leading and the trailing segments at an extrapolated mid-point time to a maneuver. The necessity for ‘tuning’ the algorithm parameters for the analysis of different objects resulting in the lack of a ‘single best set of algorithm parameters’ for all satellites is emphasized. A parameter termed as ‘time-lag’ was defined and it corresponds to the difference between the epoch of the peak of the time-series data and a known (truth) maneuver time. An average offset of around 2-3 days is reported [2] and was attributed to many factors including the latency in state estimates used for generating the TLEs, lack of post-maneuver data etc.

Ref. [3] proposed two techniques for the detection of maneuvers from TLEs, the first involves a consistency check of the time-series data from TLEs and the second is a slightly modified version of the moving window technique mentioned in [1]. The first method (TCC) is based on the notion that unless a maneuver occurs, the spatial discrepancy between the propagated state and the later published state should be small. The second method (TTSA) applies two pre-processing steps of analyzing the input time series for the detection of harmonics and estimating the noise of the time series without harmonics, before applying the moving window method. It is found that the second method (TTSA) results in less false positives compared to the first method. Ref. [4] modified the TCC method by employing a filter that leverages locally weighted regression and when applied to the pairwise differential residuals, analyzes their fundamental structure.

Ref. [5] modeled the maneuver as a jump Markov nonlinear system having multiple modes. Then an interacting multiple model estimation simulation is performed, and the mode with highest probability is correlated with the maneuver of the spacecraft. Ref. [6] developed a method to identify abnormal data segments compared to identifying outliers from the TLE data for maneuver detection. Two anomaly indices (SMA-based and inclination-based) are used to denoise the different data segments and generated using a discrete wavelet technique. All the above-mentioned literature requires thresholds to be specified for the analysis and it is well established that thresholds differ for different objects and are highly dependent on the type of data. Further, the sensitivity of these techniques to the thresholds directly decides the reliability of the maneuver detection. To reduce the outliers in the TLE data aimed at enabling an automatic detection of thresholds, Ref. [7] presented a new filter based on an Expectation Maximization algorithm. The variances estimated in the polynomial regression and prediction are used to determine the thresholds. However, in consistency with other literature, the window length and the threshold setting strategies are found to be the most

Copyright © 2024 Advanced Maui Optical and Space Surveillance Technologies Conference (AMOS) – www.amostech.com

significant parameters in the effectiveness of the algorithm. Recently, the application of AI/ML techniques for the detection of maneuvers [8] is gaining prominence but the literature is not discussed herein for brevity.

The technique for maneuver detection from raw optical observations is closely related to data association and object tagging. The advantages of such an approach will be twofold: 1) it reduces the time between occurrence and detection of the maneuver, and 2) since the measurements are directly used for maneuver detection, it does not require additional pre-processing of data in batches before it is fed into the algorithm. The underlying idea behind this approach is explained in detail in [9] which involves data association of noise-corrupted measurements to the source it originated from, followed by filtering and state estimation. Several efficient and robust multi-target tracking algorithms like the Global Nearest Neighbor (GNN) [10], Joint Probabilistic Data Association (JPDA) [11], Multiple Hypothesis Tracking (MHT) [12], Random Finite Sets (RFS) [13] have been established after rigorous implementation and testing. The associated measurements, along with a-priori states, undergo the Kalman filtering process [14], for the estimation of posterior states.

In a situation where the spatio-temporal variation of the target state is only governed by the natural forces, the track-to-orbit (T2O) correlation works effectively within a certain gating threshold. However, if the target performs a maneuver, its orbit starts receding gradually from the one computed by the standard orbit propagation dynamics. As a result, the T2O correlation stops, and the incoming measurement is then initialized as an Uncorrelated Observation (UCO) [15]. The initialization of a new UCO is attributed to two possibilities: 1) the UCO originated from the same object, but the object may have performed a maneuver, 2) the UCO originated from an object not listed in the catalog. The scope of this paper is limited to processing UCOs that originate out of a maneuver. Ref. [16] proposed a very straightforward methodology in which Mahalanobis distance was used as an indicator to detect a maneuver, followed by a conjunction analysis-based approach for its estimation. They also used an EKF/UKF framework to compute posterior state estimates, using the incoming measurements pre- and post-maneuver. However, the problem of correlation of UCO with its corresponding target still remains a major challenge if the algorithm is to be used to accommodate multiple targets simultaneously.

Based on the literature mentioned above, it can be observed that there is no common framework to derive maneuvers from different data types and attributes. Further, the quantification of the reliability of the maneuver detection algorithms remains a tough task because of many uncertainties, inconsistencies and insufficiencies in the input data, lack of truth to validate the derived maneuvers and most importantly the deliberate covert nature of maneuvers of military assets. To address these issues, the current paper proposes a multi-perspective multi-modal evaluation of the pattern of life of RSOs in LEO. The different data types such as raw optical observations, TLEs and state vectors are processed and the maneuver detection techniques for each of these data types are described. A multi-perspective post-processing is carried out to determine the purpose of the maneuver and to derive further inferences regarding maneuver reconstruction.

The paper is organized as follows: the maneuver detection from TLEs is described in the next section. The proposed ‘iterative sequential window’ method builds on the moving window method by adding one more layer of iterative analytics on the current window of data. The maneuver detection from the state vector data is described next. The fundamental characteristics of the data being very different from that of the TLEs, the moving window method is modified to account for the cyclic variation of the data. Subsequently, the technique for maneuver detection from optical observations is explained. The proposed technique is built upon a hypothesis-based tracking algorithm, where each hypothesis makes a claim about the source of measurement, based on its statistical distance with respect to the predicted measurement. Then individual analyses are correlated and post-processed to derive the purpose of the maneuver. Summary and conclusions are presented in the final section, describing the scope for future work.

3. MANEUVER DETECTION FROM TLE

3.1 Data collection and processing

The TLEs for the analysis of maneuver detection are sourced from the publicly available NORAD data through Space-Track [17] for the specified analysis timeframe. The TLE data is then categorized according to the timestamp chronologically and the Day of the Year (DOY) is used subsequently to tag the TLEs. Further, if there are multiple TLEs in a day, the difference of the parameter values between the first TLE and last TLE is also quantified. In this

Copyright © 2024 Advanced Maui Optical and Space Surveillance Technologies Conference (AMOS) – www.amostech.com

manner, the smaller variations within a day are attributed to orbital decay and the larger, significant deviations across the day are analyzed. The time-stamped data in TLE is then transformed into the classical orbital elements and the individual parameters such as Semi-Major Axis (SMA), inclination etc. are analyzed independently.

3.2 Basic moving window method

A methodology to detect maneuvers from TLEs similar to that proposed by [1] is implemented first. The analysis of each parameter derived from the TLEs begins with a curve fit of the given data to a linear polynomial curve (a linear curve fit avoids overfitting of the data). The data is divided into multiple chunks and different curve fits are established for different chunks of data. Then a moving window analysis follows. The choice of window length is an important step in the maneuver detection process and a typical value of 10 days can be used as a good initial window length when the TLE data spans more than 30 days. The next step is the computation of deviation from the actual SMA values from the TLE and the values predicted by the fitted curve. These deviations form the basis of the maneuver detection process in two ways: 1) a threshold to distinguish between the normal orbital behavior and potential maneuvers is defined based on the Mean Absolute Deviation of the computed deviations and 2) the comparison of the threshold with the actual values of deviations to flag potential maneuvers. From the definition of threshold, upper and lower limits (confidence intervals) for anomaly detection are established using a significance level (α = 0.05). The acceptance of the confidence interval can be set using the significance level. The deviations which exceed the threshold are categorized as maneuvers and the consecutive detections within a specified time frame are eliminated ensuring that each detected maneuver is unique and significant. Then the maneuver characteristics such as start, end epochs, the resulting orbital parameter change (say, change in SMA or inclination) etc. are derived.

Using the above-mentioned methodology, many RSOs in LEO were analyzed. The truth data for the maneuvers conducted by satellites being very rare (a few true maneuvers can be accessed in [19]), this research generates the truth data by visual inspection of the time history of SMA and inclinations of various RSOs similar to the approach followed in [20]. A tool is created which plots the time-series of actual parameter values and the deviations from the fitted curve. The True Positives (TP) are identified by visual inspection, denoting here on as 'truth maneuver data'. An algorithm-derived maneuver detection is classified as true positive if the maneuver epoch falls within ± 1 day from the epoch of the actual maneuver data and other detections are classified as False Positives (FP) or False Negatives (FN) depending on the comparison with actual maneuver data. These values are used to compute the $F1$ score based on the following formulae:

$$Precision = TP/(TP + FP) \tag{1}$$

$$Recall = TP/(TP + FN) \tag{2}$$

$$F1\ score = 2 * (Precision * Recall)/(Precision + Recall) \tag{3}$$

The performance of the maneuver detection algorithm in the existing literature for different RSOs are quantified in Table 1. The semimajor axis history and the detected maneuvers are presented in Fig. 1.

Table 1: Performance of the basic maneuver detection algorithm.

RSO	TP	FP	FN	$Precision$	$Recall$	$F1\ score$
581xx	13	107	2	0.10833	0.86666	0.19259
458xx	5	40	0	0.11111	1	0.2
460xx	8	42	0	0.16	1	0.27586
457xx	7	56	0	0.11111	1	0.2
558xx	4	24	7	0.14285	0.363636	0.20512

From Table 1, it can be observed that the reliability of maneuver detection performed by the existing maneuver detection algorithms is poor. The fundamental reason is the large number of false positives and stems from the inappropriate value of threshold and duplication of detected maneuvers across different windows. Based on this

Copyright © 2024 Advanced Maui Optical and Space Surveillance Technologies Conference (AMOS) – www.amostech.com

reasoning, the current research proposes an iterative sequential window method which doesn't need an explicit threshold to be described and is explained in the next section.

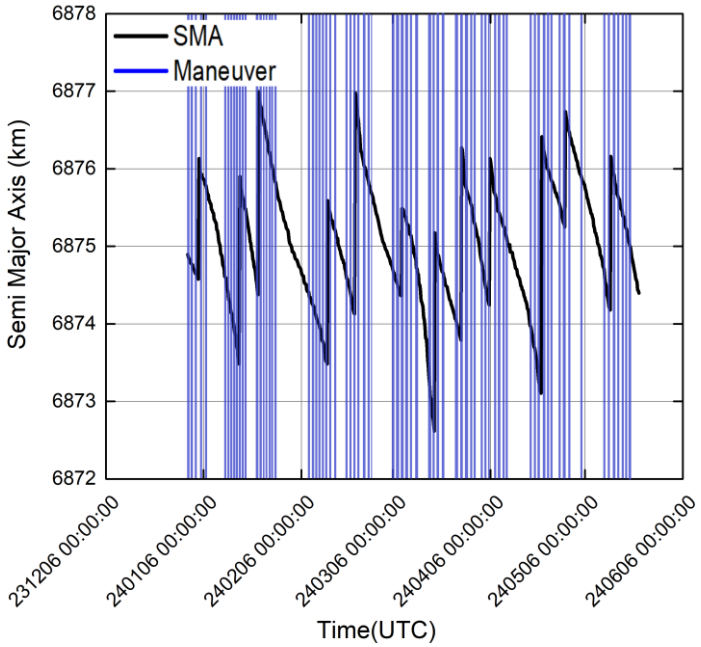

Fig. 1: Maneuver detection of object 581xx using basic moving window method.

3.3 Iterative sequential window method

The iterative sequential window method builds on the conventional moving window method by adding one more layer of analysis on the data. Within a fixed window of data, the preliminary step involves removal of the first data point from the analysis and subsequent application of moving window technique. In the next step, the second data point is removed, and the process repeats till the last data point is removed from the analysis, forming an iterative method and the standard deviations for all these window segments are computed, as depicted in Fig. 2.

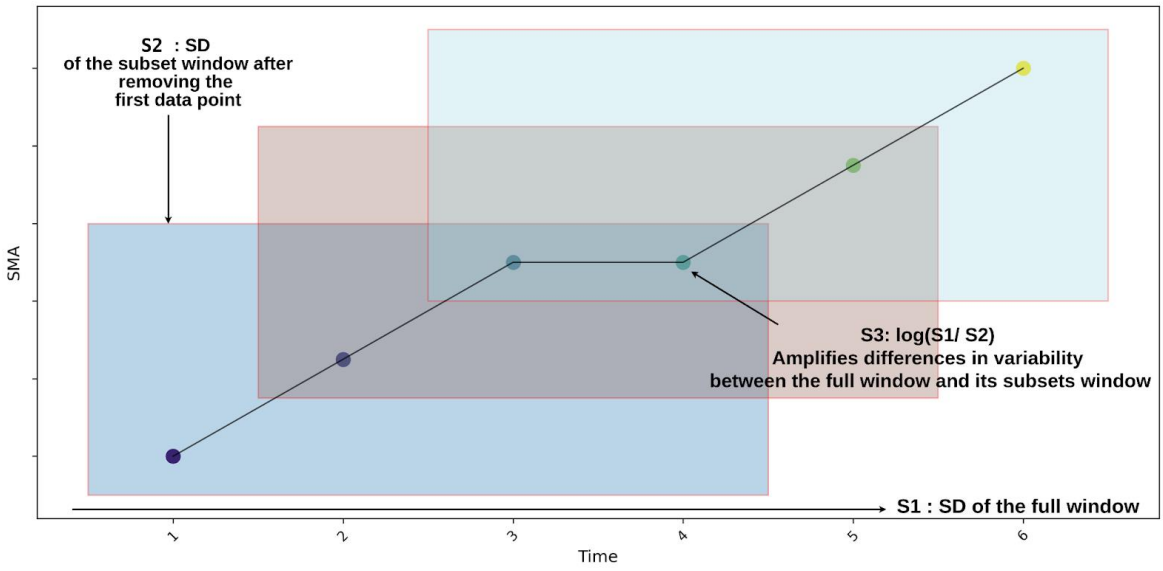

Fig. 2: Concept of iterative sequential moving window.

Copyright © 2024 Advanced Maui Optical and Space Surveillance Technologies Conference (AMOS) – www.amostech.com

The next step involves computation of a test statistic, denoted f is computed by the following formula:

$$f = log(\sigma_{ww}/\sigma_{sw}) \tag{4}$$

The test statistic f compares the standard deviation of the whole window (ww) to the average standard deviation of the subset window (sw). This magnifies a significant change in variability between the standard deviations of whole window and smaller window, eventually contributing to reject or accept the null hypothesis of maneuver. The next step in the algorithm is the computation of a Bayes factor (BF), a function of the lengths of the whole window and smaller windows, as defined below.

$$BF = NF * EF \tag{5}$$

where

$$Normalisation\ Factor\ (NF) = \frac{(N_{ww} - 2)^{3/2}}{2\sqrt{\pi(N_{ww} - 1)(N_{sw} - 1)}} \tag{6}$$

$$Exponential\ Factor\ (EF) = e^{2\left[\frac{N_{ww} - N_{sw}}{(N_{ww} + N_{sw}) - 2}\right]f - \frac{(N_{ww} - 1) * (N_{sw} - 1)}{(N_{ww} + N_{sw}) - 2}} \tag{7}$$

The normalization factor (NF) adjusts for the size of the windows. This adjustment helps maintain consistency and reliability in detecting maneuvers, regardless of how large or small the analyzed data windows are. The exponential factor (EF) is where the actual comparison happens. It uses the test statistic f and checks how the differences between the full and smaller windows compare when adjusted for their sizes. If the smaller window shows a significantly different standard deviation than the full window, the exponential term and the Bayes Factor BF will be high, suggesting that a maneuver is likely.

The last step in the iterative sequential moving window technique is the computation of the Bayesian Probability (BP). Bayesian probability helps quantify how confident that a detected change in the data is due to a maneuver rather than random fluctuations or due to orbital perturbations. A high BF means there's strong evidence for a maneuver, while a low BF suggests otherwise.

$$BP = \frac{BF * (1 - \frac{1}{winlen})}{\left(1 + BF * \left(1 - \frac{1}{winlen}\right)\right)} \tag{8}$$

The formula adjusts the Bayes Factor based on the size of the window ($winlen$). It accounts for the fact that as the window size increases, the chance of detecting a maneuver due to random noise decreases. The term $\left(1 - \frac{1}{winlen}\right)$ helps to normalize the influence of the window size. The formula ensures that the resulting BP value falls between 0 and 1, which is the standard probability range.

BP assesses the likelihood that a detected change in data is due to a maneuver rather than random noise. A BP value close to 1 suggests strong evidence that a maneuver has occurred, while a value near 0 indicates that the change is likely due to random fluctuations. The threshold for BP, which is $\frac{1}{winlen}$, decreases as the window length ($winlen$) increases, making the criterion for detecting a maneuver stricter and reducing sensitivity to minor fluctuations. Conversely, with smaller windows, the threshold is higher, increasing sensitivity and the likelihood of detecting maneuvers. Thus, if BP exceeds this threshold, it suggests a high probability that a maneuver has taken place. A high-level flow chart representing the maneuver detection using the iterative sequential window method is depicted in Fig. 3.

Copyright © 2024 Advanced Maui Optical and Space Surveillance Technologies Conference (AMOS) – www.amostech.com

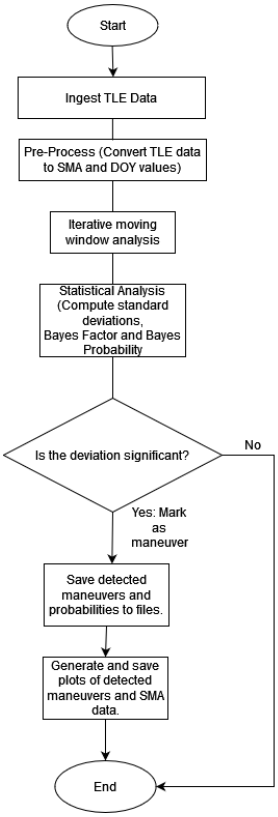

Fig. 3: High level flowchart of the maneuver detection process using iterative sequential window technique.

3.3.1 Maneuver detection from TLEs using the iterative sequential window method

The TLE data of satellites used in the previous section was used to quantify the maneuver detection performance using the iterative sequential window method and results are presented in Table 2.

Table 2: Performance of the iterative sequential window method for maneuver detection from TLEs.

RSO	TP	FP	FN	$Precision$	$Recall$	$F1\ score$	**% improvement in $F1\ score$ compared to basic method**
581xx	13	2	2	0.86666	0.86666	0.86666	350.00
458xx	5	2	0	0.71428	1	0.83333	333.33
460xx	6	0	0	1	1	1	214.29
457xx	7	2	0	0.77777	1	0.875	333.33
558xx	6	3	5	0.66666	0.545454	0.6	322.22

It can be observed from Table 2 that the performance and reliability of the iterative sequential window method is significantly greater compared to the basic moving window method. As an indicative result, the maneuver detection of the RSO 581xx for the timeframe from 01/01/2024 to 01/08/2024 is plotted in Fig. 4.

Copyright © 2024 Advanced Maui Optical and Space Surveillance Technologies Conference (AMOS) – www.amostech.com

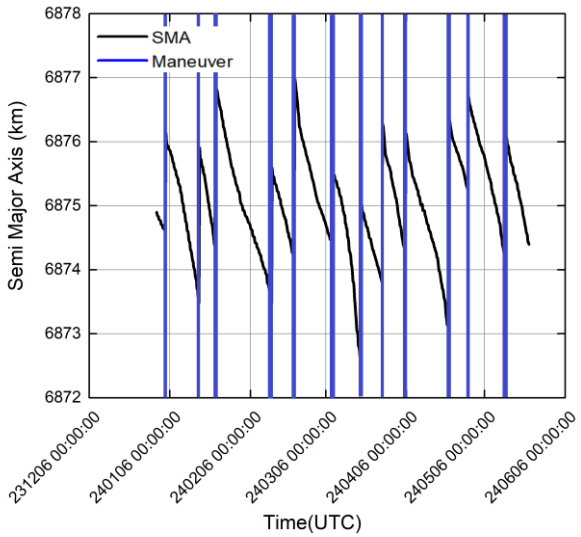

Fig. 4: Maneuver detection of the object 581xx using TLEs using the iterative sequential moving window method

During this period, this object is found to have conducted 12 along track maneuvers, ranging from SMA changes of 1.1257 km to 3.3054 km. All these maneuvers are identified to be orbit maintenance maneuvers. From the orbital evolution, the satellite is deduced to have a high thrust chemical propulsion system. The mass of the satellite (as obtained from public verified sources) is about 300 kg. The average period between each maneuver is about 17 days. The temporal distribution of these maneuvers is nearly repetitive in nature, the least duration between maneuvers being 11 days and the most duration was 28 days. Based on the pattern of maneuvers, an along track maneuver was predicted to happen around 31-07-2024 to 23-08-2024, without the knowledge of the TLEs around that time frame. When the actual orbital data was received, the satellite was found to have conducted a maneuver on 21-08-2024, confirming the hypothesis of orbit maintenance maneuvers.

As another demonstration of the maneuver detection and an associated purpose, the SMA history of the satellite 558xx is presented in Fig. 5. This satellite has conducted a rigorous orbit maintenance with SMA 7583.925 km by orbit maintenance maneuvers at regular intervals of 30-40 days. An out of pattern maneuver was detected on 02-08-2024 between 15:00:00 UTC and 20:30:00 UTC, reflecting an SMA change of about 175m. This is correlated with a conjunction analysis of this object (generated with an in-house tool) where a close proximity with the object 394xx was observed at 07-08-2024 20:41:00 UTC. The miss distance was 1.28808 km, and the collision probability was 2.99598591e-04 (analyzed using Alfano Max Probability method [19] The subsequent analysis using data on 03-08-2024 revealed that the predicted close approach was no longer a threat. This sudden change in predicted miss distance is attributed to a maneuver on 02-08-2024 15:00:00. The secondary object did not perform any maneuvers during this period, which further confirms the inference that the observed SMA change was due to a collision avoidance maneuver (CAM) conducted by the object 558xx.

Copyright © 2024 Advanced Maui Optical and Space Surveillance Technologies Conference (AMOS) – www.amostech.com

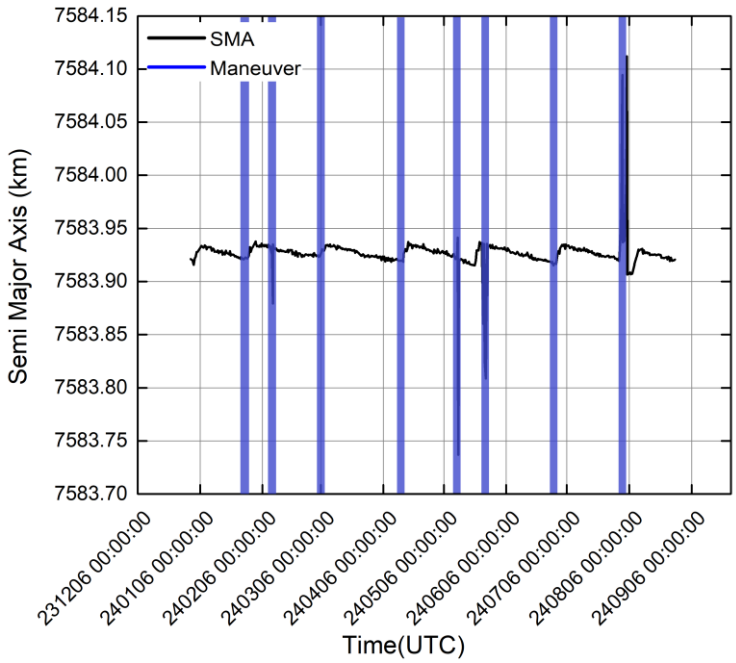

Fig. 5: Maneuver detection of 558xx using the iterative sequential window method

4. MANEUVER DETECTION FROM STATE VECTORS

Maneuver detection from state vectors is different from maneuver detection from TLEs in several aspects. First, the time series TLE data is discrete in nature whereas the state vector data is more continuous. Second, the effect of maneuver(s) on the SMA, inclination etc. are less distinguishable compared to the TLEs. Further, the grouping of the data based on timestamp of the TLE expressed as DOY will not work for the state vectors where precise timestamps are to be ingested.

4.1 Data generation and processing

The data for maneuver detection from state vectors is generated using an in-house high fidelity numerical propagator. The reason for the use of synthetic data is the unavailability of reliable open-source data for the satellite of interest (581xx). Using the information of propulsion system characteristics from the previous section and deriving the initial states from in-house proprietary data sources, two along-track maneuvers are simulated within a span of 12 hours. Each of these maneuvers spanned 8 seconds and the details are mentioned in Table 3.

Table 3: Details of maneuvers used for generating synthetic data of maneuver detection from state vectors

Maneuver	Start epoch	End epoch	Acceleration components in RSW coordinate frame (m/s^2)	Burn duration
1	2024-06-21 09:59:55	2024-06-21 10:00:00	0.0, 0.1666, 0.0	5 seconds
2	2024-06-21 21:59:55	2024-06-21 22:00:00	0.0, 0.1666, 0.0	5 seconds

Copyright © 2024 Advanced Maui Optical and Space Surveillance Technologies Conference (AMOS) – www.amostech.com

4.2 Maneuver detection from state vectors using iterative sequential window method

The maneuvers simulated in the previous section were exactly captured using the iterative sequential window algorithm. The increase in SMA due to the two maneuvers are found to be 1.540 km and 1.496 km because of the first maneuver and second maneuver respectively. Fig. 6 depicts the evolution of SMA over time and the detected maneuvers from the state vector data.

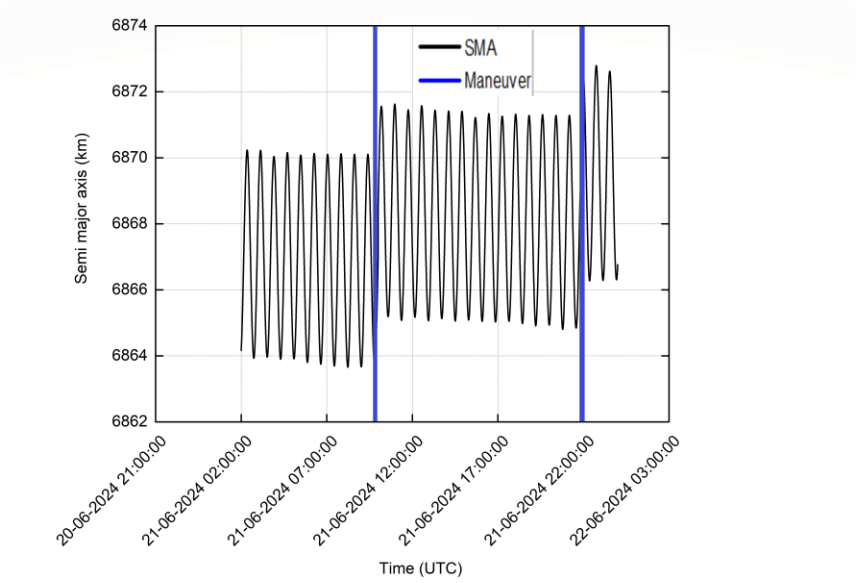

Fig. 6: Detection of maneuvers from state vectors using the iterative sequential window method

4.3 Comparison of maneuver detection from state vectors and TLEs

To compare the fidelity of maneuver detection using state vector data with the maneuver detection using TLEs, the state vector data is used to generate TLEs using an in-house developed algorithm and analysed using the iterative sequential window method. The state vector data is chunked into multiple data sets and the TLEs are generated for chunks of data not involving any maneuvers. These TLEs are then used as input for the iterative sequential window algorithm.

The TLE-based maneuver detection did not distinguish between the two maneuvers and was captured as a single large maneuver as depicted in Fig. 7. The possible reasons are twofold: 1) the maneuvers are separated temporally by just 12 hours. The sensitivity aspect of the TLE-based algorithm to detect closely conducted maneuvers is to be investigated and 2) the window length of 10 days used for the analysis is too large for the detection of closely conducted maneuvers. However, it is demonstrated that the underlying problem of maneuver detection of closely spaced maneuvers (within a few hours) can be solved by state vector-based analysis.

Copyright © 2024 Advanced Maui Optical and Space Surveillance Technologies Conference (AMOS) – www.amostech.com

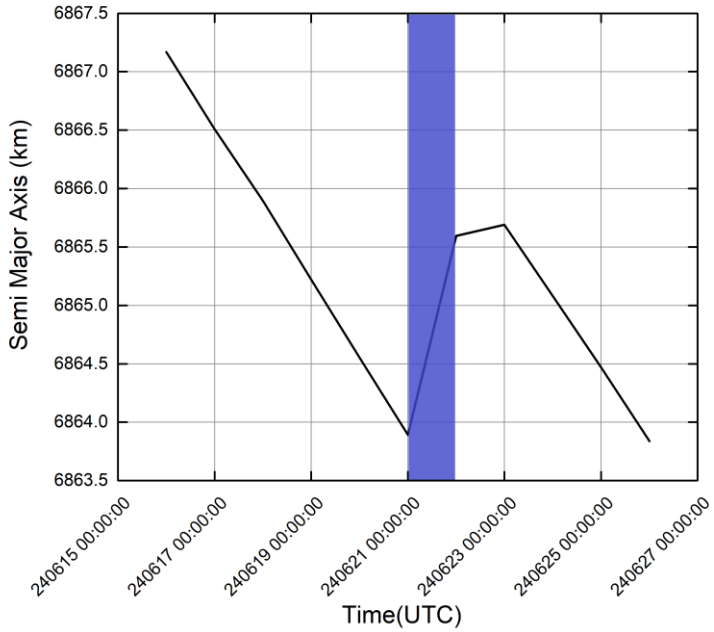

Fig. 7: Maneuver detection using TLEs generated from state vectors.

5. MANEUVER DETECTION FROM OPTICAL SENSOR OBSERVATIONS

This section describes maneuver detection from raw optical sensor observations like Azimuth & Elevation (Az, El) or Right Ascension & Declination (RA, Dec). In order to reduce latency between the execution and detection of the maneuver, insights are needed to be drawn in real time before post-processing the observations into state vectors or orbital elements. The observations data needed to perform the analysis is generated using the state vectors mentioned in the previous section.

5.1 Data generation and processing

The algorithm requires 3 data inputs: 1) the initial state of the target of interest 2) the ground station coordinates and 3) the angles-only tracking data. The first two inputs can be extracted from proprietary data sources. For angles-only tracking data, synthetic data was generated by propagation of states using an in-house high-fidelity numerical orbit propagator. The initial states were propagated till the maneuver was to be performed, then after adding maneuver, the resulting states were again propagated till the end of the astrometric scan. Besides compensating for unavailability of reliable data for the target of interest, it also allows us to generate tracking datasets with desired maneuver parameters, namely, the time of maneuver, the thrust and the duration of burn. The data was then fed into a multi-target tracking algorithm equipped with new track initialization feature, the testing conditions of which are tabulated below:

Copyright © 2024 Advanced Maui Optical and Space Surveillance Technologies Conference (AMOS) – www.amostech.com

Table 4: Simulation parameters for the multi-target tracking algorithm

Feature	Attribute
Coordinate Frame (for state vector)	TEME
Propagation model (for data association)	Two-body (Keplerian)
Initial State Covariance (P_0)	$\sigma_x = \sigma_y = \sigma_z = 1\ km$ $\dot{\sigma}_x = \dot{\sigma}_y = \dot{\sigma}_z = 10\ m/s$
Process Noise (Q)	$\sigma_x = \sigma_y = \sigma_z = 1\ m$ $\dot{\sigma}_x = \dot{\sigma}_y = \dot{\sigma}_z = 1\ cm/s$
Measurement Noise (R)	$\sigma_\alpha = \sigma_\delta =$ $5\ arc\ seconds$
Measurement step-size	5 seconds
Initial epoch for the scan	2024-06-10 12:00:00 (UTC)
Terminal epoch for the scan	2024-06-10 12:30:00 (UTC)
Upper bound threshold d_{mahal} for H_1	12

5.2 Standard target-tracking approach: Mahalanobis distance calculation

Assuming no control input, the state dynamics is modeled as:

$$x_{k+1|k} = F_k x_k + w_k \tag{9}$$

where F_k is the state transition matrix, x_k is the posterior state estimate at timestep k, w_k is the process noise, assumed to be zero-mean Gaussian with noise covariance Q. The initial state is assumed to follow a Gaussian distribution as:

$$X_0 \sim \mathcal{N}(x_0, P_0) \tag{10}$$

where x_0 is the mean state, and P_0 is the 6×6 state covariance matrix. Similarly, the relation between state and measurement can be modeled as:

$$z_k = H_k x_k + v_k \tag{11}$$

where $z_k = [\alpha_k \quad \delta_k]^T$ is the angles-only measurement pair, namely Azimuth (α) and Elevation (δ). H_k is the measurement model, and v_k is the measurement noise, also assumed to be zero-mean Gaussian with noise covariance R. In a real-time scenario, the incoming measurements z_k cannot be computed accurately by $H_k x_k$, hence another quantity called innovation or measurement pre-fit residual is calculated as:

$$\tilde{y}_k = z_k - H_k x_{k|k-1} \tag{12}$$

Using this innovation, the Mahalanobis distance is calculated as:

Copyright © 2024 Advanced Maui Optical and Space Surveillance Technologies Conference (AMOS) – www.amostech.com

$$d_{mahal} = \tilde{y}^T S^{-1} \tilde{y} \tag{13}$$

where S is the innovation covariance matrix, or the covariance of the apriori measurement pdf. The d_{mahal} is then used for hypothesis selection. Once the hypothesis is chosen, the quantity $\tilde{y}_k$, along with other quantities is used in the filtering step to get the posterior state estimates.

5.3 Hypothesis-based multi-target tracking

The technique used in this paper closely follows [16] where Mahalanobis distance is used as an indicator to detect a maneuver footprint. However, the methodology proposed by [15] also highlights the importance of track-to-orbit correlation, so that the incoming measurements can be used by UKF to get an accurate estimate of the posterior state vector of the target even after maneuver has been performed. This track-to-orbit correlation is usually carried out under a data association framework like GNN or JPDA [10-11], however, these techniques are also equipped with a certain permissible limit for association, known as gating condition. Gating condition ensures that only the measurements originated because of standard orbit propagation get associated to the orbit. Measurements originated after anomalous target activities like a maneuver, fail to satisfy these gating conditions, thus rendered uncorrelated. To evade this, a hypothesis-based tracking approach has been used. In this paper, we assume the following set of hypotheses for a measurement:

$\mathcal{H}_0$: Measurement originated from a catalogued object because of orbit propagation.
$\mathcal{H}_1$: Measurement originated from a catalogued object, because of maneuver.
$\mathcal{H}_2$: Measurement originated from a new object.

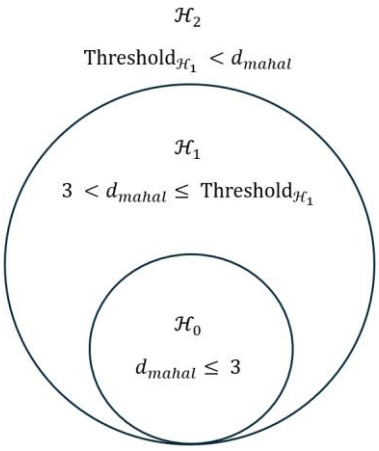

Fig. 8: Criteria for selection of measurement origin hypotheses: standard orbit propagation, maneuver and new track initiation

The rule for choosing any hypothesis is depicted in Fig. 8. Here, d_{mahal} is the Mahalanobis distance of the obtained measurement with respect to the a-priori measurement pdf. A threshold of 3 was chosen for $\mathcal{H}_0$ because a Gaussian random variable is likely to fall within 3σ-bound with a probability of over 99.7%. A calculated estimate of threshold value for $\mathcal{H}_1$ can also be decided based on the knowledge of the most aggressive maneuver the target may perform which, in turn, is an attribute to the kind of propulsion system used in the target object.

5.3.1 Maneuver detection using one-layer gating condition

Two test cases were prepared, each consisting of one maneuver performed during the 30-minute scan window, the parameters of which are presented in Table 5:

Copyright © 2024 Advanced Maui Optical and Space Surveillance Technologies Conference (AMOS) – www.amostech.com

Table 5: Details of maneuvers used for generating synthetic data of maneuver detection from observations

Maneuver	Start epoch	End epoch	Acceleration components in RSW frame (m/s^2)	Thrust
1	2024-06-10 12:15:00	2024-06-10 12:15:02	0.0, 0.1666, 0.0	50 N
2	2024-06-10 12:15:00	2024-06-10 12:15:02	0.0, 0.0333, 0.0	10 N

Data association was performed, first, with only the 3σ-bound, i.e., only the hypotheses $\mathcal{H}_0$ and $\mathcal{H}_2$. In that case, the T2O correlation stops after the detected maneuver epoch, thus indicating a maneuver, however the incoming measurement gets initialized as a new track. Fig. 7a and Fig. 7b depict the evolution of measurement pre-fit and post-fit residuals for Azimuth & Elevation separately, along with the demarcation of true and detected time of maneuver. Measurement post-fit residual is obtained by calculating the difference between incoming measurement z_k and posterior state estimate $x_{k|k}$ converted to measurement space. Because the T2O correlation stopped, the incoming measurement could not be used by the UKF for posterior state estimation, hence, the measurement post-fit residual comes out to be the same as the measurement pre-fit residual.

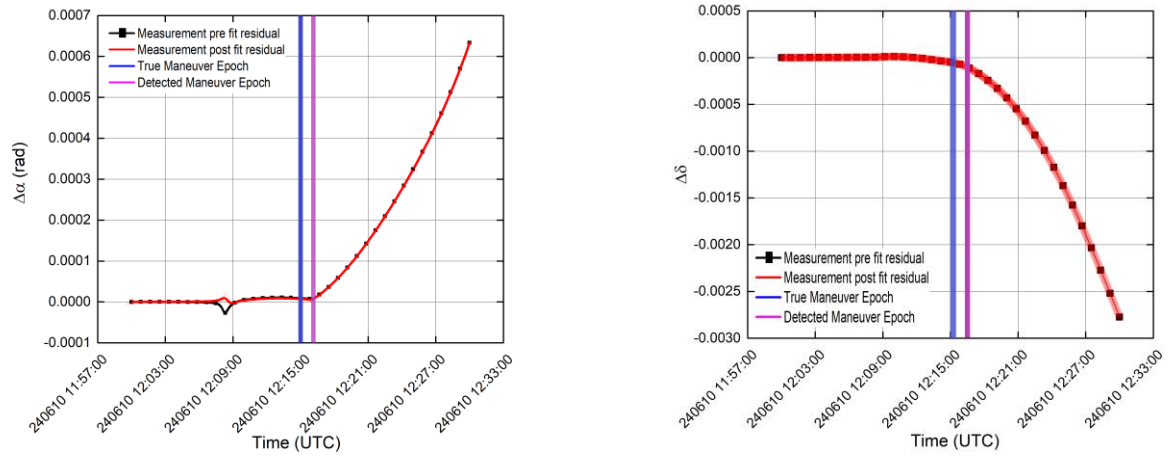

Fig. 7a: Evolution of residuals in Azimuth (left panel) and Elevation (right panel) for NORAD ID 581xx. Thrust = 50 N, Burn duration = 2 s

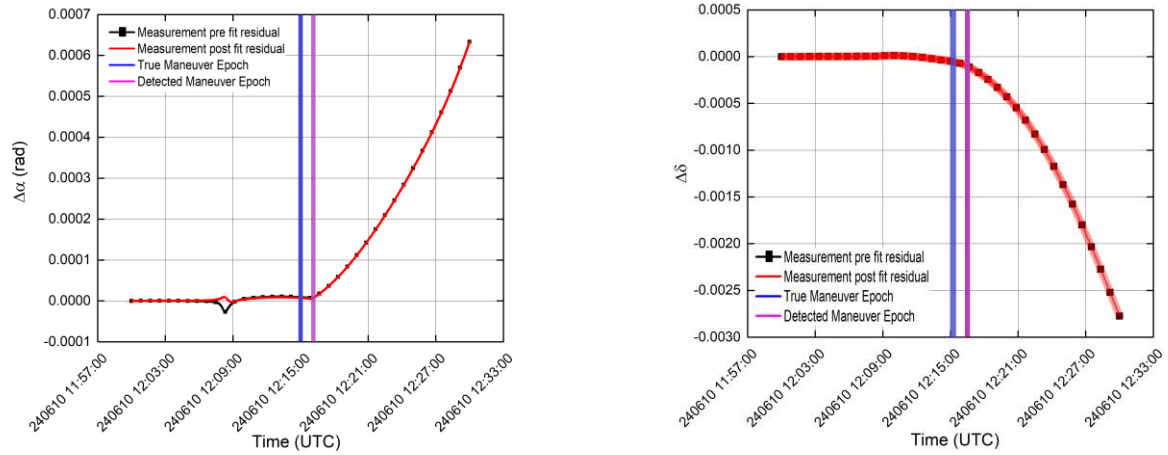

Fig. 7b: Evolution of residuals in Azimuth and Elevation for NORAD ID 581xx. Thrust = 10 N, Burn duration = 2 s

Copyright © 2024 Advanced Maui Optical and Space Surveillance Technologies Conference (AMOS) – www.amostech.com

5.3.2 Maneuver detection using two-layer gating conditions

The above process was repeated, this time, with all the 3 hypotheses $\mathcal{H}_0$, $\mathcal{H}_1$ and $\mathcal{H}_2$, i.e., with both 3σ- and 12σ-bounds. As the Mahalanobis distance exceeds 3, a maneuver is indicated, however, since it is less than 12, it can still be associated with the target. Hence, the incoming measurement is now available to be used by UKF for posterior state estimation. Fig. 8a and Fig. 8b depict a significant reduction in the measurement post-fit residual, highlighting that the filtered state is being calculated as a result of both the standard propagation and the maneuver.

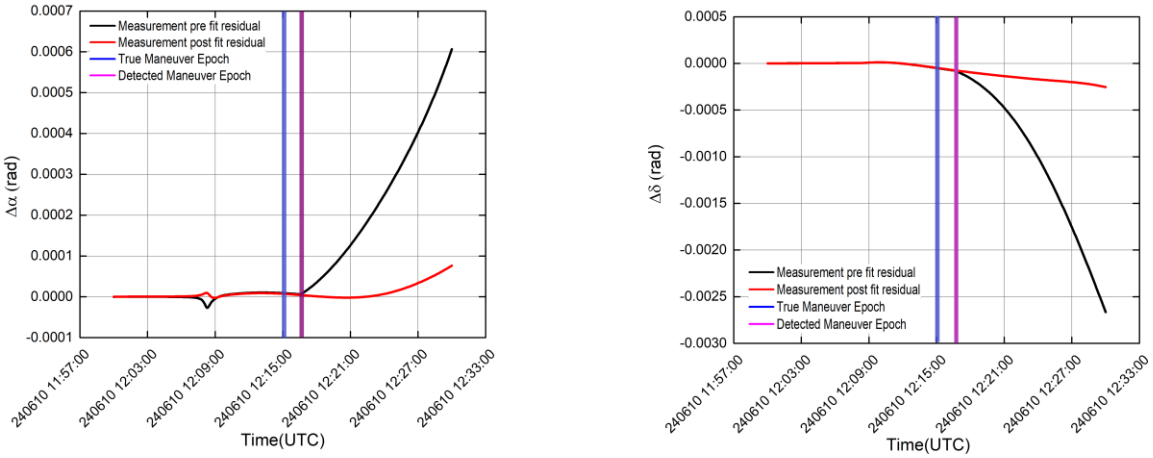

Fig. 8a: Evolution of residuals in Azimuth and Elevation for NORAD ID 581xx.
Thrust = 50 N, Burn duration = 2 s

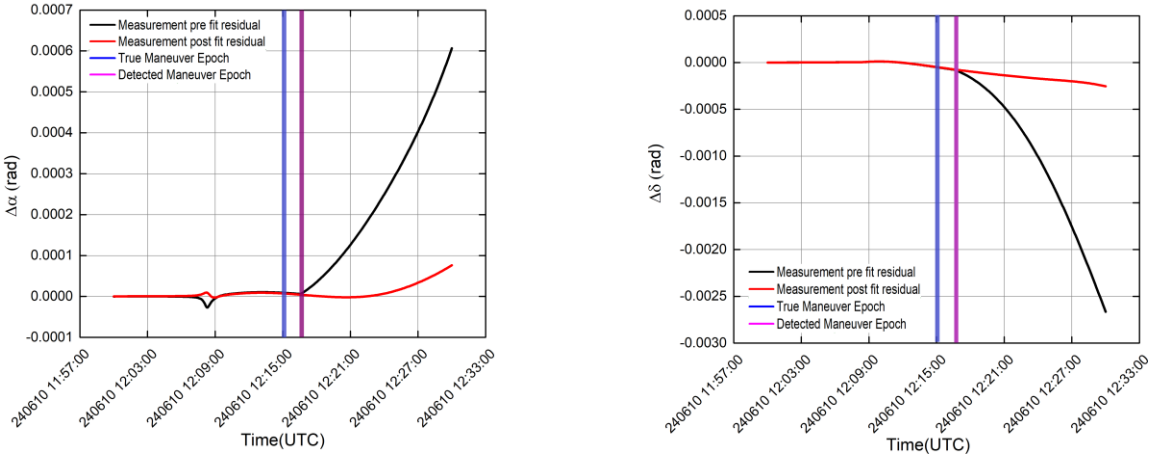

Fig. 8b: Evolution of residuals in Azimuth and Elevation for NORAD ID 581xx.
Thrust = 10 N, Burn duration = 2 s

The following plot shows the evolution of Mahalanobis distance for target tracking scenarios with Maneuver 1 and 2 respectively. Although d_{mahal}exceeds 3 at the same time for both one-layer and two-layer gating, its value diverges with time for the one-layer gating, showing a slow recession of the propagated orbit from the actual one. However, two-layer gating enables the use of UKF, which prevents the Mahalanobis distance from diverging, thus providing a more accurate state estimation after the maneuver. The improved technique based on two-layer gating condition, along with maneuver detection, solves the problem of correlation of post-maneuvered track to its pre-maneuvered orbit. This improvisation would be helpful when multiple targets perform maneuvers during the scan.

Copyright © 2024 Advanced Maui Optical and Space Surveillance Technologies Conference (AMOS) – www.amostech.com

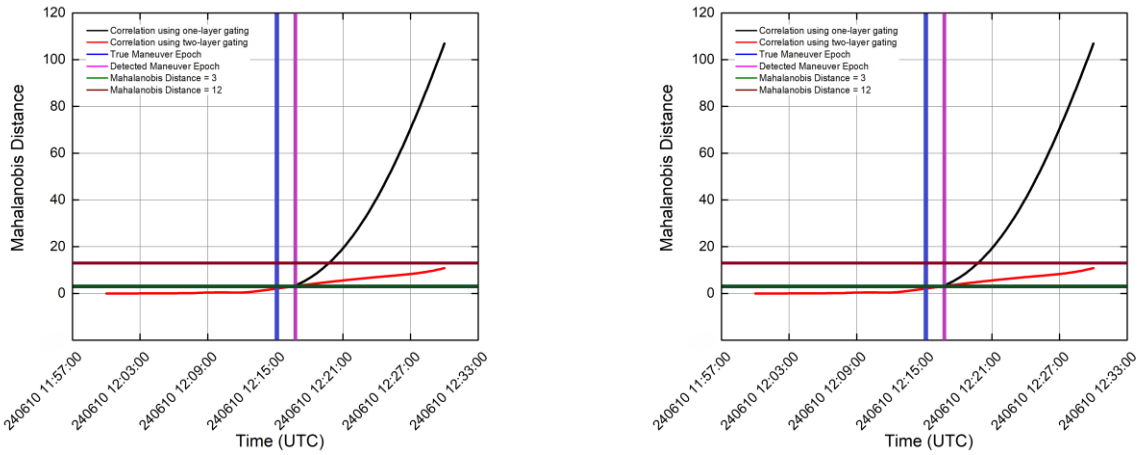

Fig. 9: Evolution of Mahalanobis distance in the two maneuver datasets for NORAD ID 581xx

Table 6: Deviation in maneuver epochs from the synthetic data generated for the two test cases

Maneuver	Thrust	True epoch	Detected epoch	Latency in detection (seconds)
1	50 N	2024-06-10 12:15:00	2024-06-10 12:16:00	60
2	10 N	2024-06-10 12:15:00	2024-06-10 12:16:30	90

Table 6 clearly shows that a more aggressive maneuver is detected with less latency than a less aggressive maneuver. Furthermore, the computation time for each maneuver and with both single-layer and double-layer gating achieved a runtime of ~7.5 minutes, thus showcasing its ability to be used for real-time data processing.

6. CONCLUSIONS

A dynamic and robust methodology to precisely characterize and synthesize PoL of satellites in LEO based on a multi-perspective multi-modal analysis is proposed. This involves a two-stage processing where the first step involves a comprehensive maneuver detection process and the second step consists of correlating, synthesizing and deriving inferences from a number of SDA related aspects. In the first stage, two new techniques for maneuver detection from optical observations and TLEs are proposed. The maneuver detection from observations is based on a hypothesis-based tracking algorithm and from the TLEs is an improvement to the moving window analysis. The proposed technique for maneuver detection from TLEs, called iterative sequential moving window method, improves the performance and reliability of the maneuver detection process by two orders of magnitude compared to a basic moving window analysis. The technique is extended to derive maneuvers from state vectors and the reliability of the inferences is found to be better compared to the maneuver detection from TLEs. The proposed technique for maneuver detection from observations is found to be compatible with near-real time processing of optical observations. In the second stage of the proposed methodology, the purpose of the detected maneuvers is derived and demonstrated for routine orbit maintenance maneuvers and a collision avoidance maneuver. The applications of the proposed methodology and the techniques developed for the characterization of space objects involve efficient and unambiguous cataloging of space objects, precise maneuver characterization and the generation of predictive analytics enabling reliable, action-oriented space domain awareness.

Copyright © 2024 Advanced Maui Optical and Space Surveillance Technologies Conference (AMOS) – www.amostech.com

7. REFERENCES

[1] Patera, R. P. (2008). Space event detection method. *Journal of Spacecraft and Rockets, 45*(3), 554–559.

[2] Kelecy, T., Mitchell, D., & Johnson, W. (2007). Satellite maneuver detection using Two-line Element (TLE) data. In *Proceedings of the Advanced Maui Optical and Space Surveillance Technologies Conference* (pp. 1-10). Maui Economic Development Board (MEDB).

[3] Lemmens, S., & Krag, H. (2014). Two-line-elements-based maneuver detection methods for satellites in low Earth orbit. *Journal of Guidance, Control, and Dynamics, 37*(3), 860–868.

[4] Zhao, Y., Smith, J., & Brown, A. (2014). A method for improving two-line element outlier detection based on a consistency check. In *Proceedings of the Advanced Maui Optical and Space Surveillance Technologies Conference* (pp. 1-10). Maui Economic Development Board (MEDB).

[5] Lee, S., & Hwang, I. (2015). Interacting multiple model estimation for spacecraft maneuver detection and characterization. In *Proceedings of the AIAA Guidance, Navigation, and Control Conference*. American Institute of Aeronautics and Astronautics.

[6] Li, T., Li, K., & Chen, L. (2018). New manoeuvre detection method based on historical orbital data for low Earth orbit satellites. *Advances in Space Research, 62*(3), 554–567.

[7] Liu, J., Zhang, Y., & Wang, X. (2021). TLE outlier detection based on expectation maximization algorithm. *Advances in Space Research, 68*(7), 2695–2712.

[8] Bai, X., Zhang, Y., & Liu, J. (2019). Mining two-line element data to detect orbital maneuver for satellite. *IEEE Access, 7*, 129537–129550.

[9] Bar-Shalom, Y., & Li, X.-R. (1995). *Multitarget-multisensor tracking: Principles and techniques* (Vol. 19). YBS Publishing.

[10] Petsios, M. N., Alivizatos, E. G., & Uzunoglu, N. K. (2008). Solving the association problem for a multistatic range-only radar target tracker. *Signal Processing, 88*(9), 2254–2277

[11] Kaufman, E., Lovell, T. A., & Lee, T. (2016). Minimum uncertainty JPDA filters and coalescence avoidance for multiple object tracking. *The Journal of the Astronautical Sciences, 63*(2), 308–334.

[12] Blackman, S. S. (2004). Multiple hypothesis tracking for multiple target tracking. *IEEE Aerospace and Electronic Systems Magazine, 19*(1), 5–18.

[13] Vu, T. (2016). A new type of random finite set for multi-target tracking. In *Proceedings of the 2016 IEEE International Conference on Multisensor Fusion and Integration for Intelligent Systems (MFI)* (pp. 1–6). IEEE.

[14] Julier, S. J., & Uhlmann, J. K. (1997). New extension of the Kalman filter to nonlinear systems. In *Signal processing, sensor fusion, and target recognition VI* (Vol. 3068, pp. 182–193). SPIE.

[15] A. Pastor, G. Escribano, M. Sanjurjo-Rivo, and D. Escobar, "Satellite maneuver detection and estimation with optical survey observations," *The Journal of the Astronautical Sciences*, vol. 69, no. 3, pp. 879–917, Jun. 2022.

[16] C. M. Bergmann, A. Zollo, J. Herzog, and T. Schildknecht, "Integrated manoeuvre detection and estimation using nonlinear Kalman filters during orbit determination of satellites," *8th European Conference on Space Debris*, May 2021.

[17] "Space-Track.org." Accessed: Aug. 22, 2024. [Online]. Available: https://www.space-track.org/auth/login

[18] "ILRS | Data and Products | Satellite Predictions | maneuver." Accessed: Aug. 22, 2024. [Online]. Available: https://ilrs.gsfc.nasa.gov/data_and_products/predictions/maneuver.html

[19] Song, W. D., Wang, R. L., & Wang, J. (2012). A simple and valid analysis method for orbit anomaly detection. *Advances in Space Research, 49*(2), 386–391

[20] Alfano, S. (2005). Relating position uncertainty to maximum conjunction probability. *The Journal of the Astronautical Sciences, 53*(2), 193–205.

Copyright © 2024 Advanced Maui Optical and Space Surveillance Technologies Conference (AMOS) – www.amostech.com